IEEE Access
Multidisciplinary | Rapid Review | Open Access Journal

Received April 23, 2020, accepted May 6, 2020, date of publication May 11, 2020, date of current version May 27, 2020.

Digital Object Identifier 10.1109/ACCESS.2020.2993897

Planar Four-Port Dual Circularly-Polarized MIMO Antenna for Sub-6 GHz Band

SHOBHIT SAXENA[1], BINOD KUMAR KANAUJIA[2], SANTANU DWARI[1], SACHIN KUMAR[3], HYUN CHUL CHOI[3], AND KANG WOOK KIM[3]

[1]Department of Electronics Engineering, IIT (ISM), Dhanbad 826004, India
[2]School of Computational and Integrative Sciences, Jawaharlal Nehru University, New Delhi 110067, India
[3]School of Electronics Engineering, Kyungpook National University, Daegu 41566, South Korea

Corresponding author: Kang Wook Kim (kang_kim@ee.knu.ac.kr)

This work was supported in part by the National Research Foundation (NRF) of Korea funded by the Ministry of Education, Science, and Technology through the National Research and Development Program under Grant NRF-2019M1A7A1A03088464, and in part by the BK21 Plus Project funded by the Ministry of Education, South Korea, under Grant 21A20131600011.

ABSTRACT In this work, two configurations (Config.-A and Config.-B) of planar four-port dual circularly-polarized (CP) multiple-input-multiple-output (MIMO) antenna are proposed for sub-6 GHz (3.4–3.8 GHz) applications. The MIMO antennas are designed on the FR-4 substrate with size of $60\times60\times1.6$ mm^3. Each radiating element (unit cell) of the MIMO antenna is comprised of a microstrip feed line and an open slot ground plane integrated with two rectangular arms for realizing circular polarization. An I-shaped metallic strip is used in the proposed four-port MIMO Config.-A and Config.-B antennas for obtaining common voltage level in the ground plane. Both MIMO antenna configurations exhibit good impedance matching in the band of interest. In the MIMO Config.-A antenna, all ports provide the same CP band, while in the Config.-B antenna the ports-1/-2 and -3/-4 radiate at different CP bands. The proposed MIMO Config.-A and Config.-B antennas support both types of polarization (left-hand circular polarization (LHCP) and right-hand circular polarization (RHCP)). With the Config.-B antenna, the maximum 3-dB axial-ratio (AR) beamwidths of 118.9° and 92.7° are obtained at 3.536 GHz in the *xz*- and *yz*-planes, respectively. Furthermore, the I-shaped strip helps in improving 3-dB AR beamwidth in the MIMO Config.-B antenna. Inter-element isolation greater than 19 dB and envelope correlation coefficient (ECC) less than 0.12 (far-field) are achieved between the ports of the fabricated MIMO antenna prototype.

INDEX TERMS Connected ground, dual circular polarization, four-port, MIMO antenna, planar.

I. INTRODUCTION

The multiple antenna elements at the transmitter and receiver end upsurge the channel capacity, data transmission rate, and quality of the wireless communication system. Adopting more number of antenna elements within a receiving system improves the link reliability of the radio receiver [1]–[2]. However, the limited space available at the communication terminals increases the problem of mutual coupling, thus deteriorating the overall performance of the system [3]. The multiple-input-multiple-output (MIMO) antenna using polarization diversity resolve this issue of mutual coupling [4]. The correlation among antenna elements can be reduced by locating the radiators in the horizontal and vertical orientation without introducing any complex decoupling structure between antenna unit cells. Recently, a number of MIMO/diversity antennas with a different arrangement of radiators for achieving polarization diversity have been reported [5]–[8]. A quad-port MIMO antenna with radiating elements wrapped around four sides of the cuboidal polystyrene block was presented in [5]. A reconfigurable shared aperture MIMO antenna with a horizontal and vertical arrangement of radiating elements was proposed in [6]. In [7], a 3-D array comprised of eight antenna elements with four-elements vertically located, and remaining four horizontally placed was presented. However, the reported MIMO antennas in [5]–[7] were non-planar designs with complex architecture and relatively bulky size. In [8], a planar quasi-self-complementary MIMO antenna composed of two-/four-port was presented for polarization diversity.

It is observed that the polarization diversity in MIMO antennas presented in [5]–[8] was realized by using

The associate editor coordinating the review of this manuscript and approving it for publication was Kwok L. Chung.

linearly-polarized (LP) antenna elements. However, compared to LP radiators, circularly-polarized (CP) antenna elements exhibit several significant advantages in terms of radio wave propagation. For example, CP antennas effectively alleviate the multipath fading effects and are also robust to polarization mismatch [9], [10]. Furthermore, the strength of the electromagnetic (EM) signals received at the wireless terminals is relatively constant, irrespective of the CP antennas orientation [11], [12]. These properties of CP antennas make them potential candidates for the upcoming MIMO wireless systems.

In the last decade, a few CP MIMO/diversity antenna structures have been proposed for WLAN, C-band, and satellite navigation applications [13]–[16]. A planar two-port CP MIMO antenna comprised of upper and lower radiators physically separated by a distance equal to the thickness of the substrate material was presented in [13]. In [14], a planar three-element MIMO antenna for achieving both pattern and polarization diversity was reported. In [15], a four-port multi-layered antenna with two radiating patches and frequency selective surface (FSS) superstrate for the generation of CP waveform was reported, which would be difficult to be integrated with other monolithic microwave integrated circuits (MMICs) in portable devices. A planar four-port CP MIMO antenna with corner truncated patches was presented in [16] for Wi-MAX/WLAN applications. The CP MIMO antennas in [13]–[16] can generate either left-hand circularly-polarized (LHCP) waves or right-hand circularly-polarized (RHCP) waves.

The MIMO antennas capable of generating dual-CP waves (both LHCP and RHCP) at the same frequency are in huge demand these days since these antennas can significantly reduce the mutual coupling and multipath fading effects [17], [18]. In the literature, some planar two-port dual-CP MIMO antennas radiating both LHCP and RHCP waves simultaneously have been reported [19]–[21]. In [19], a two-port coplanar waveguide (CPW)-fed planar antenna composed of two asymmetric T-shaped feed lines was presented for dual circular polarization. A broadband dual-CP two-port antenna with L- and inverted L-shaped strips on the radiating edges of the monopole was presented in [20], where the antenna was excited by dual orthogonal microstrip lines. In [21], two CPW feeds were utilized for realizing dual circular polarization. The link reliability in wireless systems can be further improved by designing dual-CP MIMO antennas with more than two radiating elements.

Furthermore, a detailed discussion related to the importance of the connected (single) ground plane in MIMO antennas was presented in [22]. The MIMO antennas must have a common ground plane to possess equal reference voltage level. The planar antennas proposed in [16], [20] does not have a common ground plane, and hence might not be used in practical applications. The same can be said for the non-planar designs proposed in [5]–[7] since those antennas also have separated ground planes. Since there is no current coupling, high inter-element isolation levels were reported in such MIMO structures (like isolation >37 dB in [16]). The two-/three-port CP/dual-CP planar MIMO antennas proposed in [14], [19], and [21] can be used in practical systems since they have a single reference voltage level (common ground plane).

It is quite challenging to retain circular polarization characteristics of the antenna elements (unit cells) in the ground radiating CP MIMO structures when the ground planes are connected. The 3-dB axial-ratio (AR) beamwidth of the MIMO antenna is also an important factor, and a wide 3-dB beamwidth is required for efficient functioning of the antenna. In this article, an attempt has been made to address all the above-stated issues. The main contributions are:

- Two planar four-port dual-CP MIMO antenna configurations (Config.-A and Config.-B) are designed for sub-6 GHz (3.4–3.8 GHz) applications. Both of the antennas radiate RHCP waves when ports-1 and -4 are excited, and LHCP waves when ports-2 and -3 are excited.
- In the MIMO Config.-A antenna, all the radiating elements provide the same 3-dB axial-ratio bandwidths (ARBWs) of ∼240 MHz. However, the 3-dB band can be easily varied by varying the arm length (m) of the CP radiator if required.
- In the MIMO Config.-B antenna, the arm length of the CP radiator is changed in such a way that port-1/-2 and port-3/-4 radiate at different CP bands. As a result, the antenna covers the entire 3.4–3.8 GHz bandwidth.
- An equal reference voltage level is obtained in the ground plane of the proposed MIMO antenna by making use of an I-shaped strip.
- It is also shown that the I-shaped strip plays an important role in improving the 3-dB AR beamwidth (in both xz- and yz-planes) of the MIMO Config.-B antenna.

II. ANTENNA CONFIGURATION

A. DESIGN OF A CIRCULARLY-POLARIZED ANTENNA ELEMENT

A CP single antenna element (unit cell) is designed on the FR-4 substrate (with relative permittivity of 4.4 and loss tangent of 0.02) of size $25\times25\times1.6$ mm^3. A 3-D EM simulator, ANSYS HFSS, is used for antenna design. The schematic of the unit cell is shown in Fig. 1, and its design parameters are stated in Table 1.

The evolution steps of the unit cell are presented in Fig. 2. Firstly, a wide hexagonal slot is introduced in the ground plane of the square-shaped antenna element, shown in Fig. 2(a). The hexagonal wide-slotted ground plane geometry (step-1) is inspired by the design proposed by the author's group in [4]. In design step-1, the width of the metal boundaries is sufficient enough for the formation of the current closed loop. The center frequency (f_c) of the unit cell is evaluated as [23]

$$f_c = \frac{c}{(x_5 + \Delta L)\sqrt{\varepsilon}_{r_{eff}}} \tag{1}$$

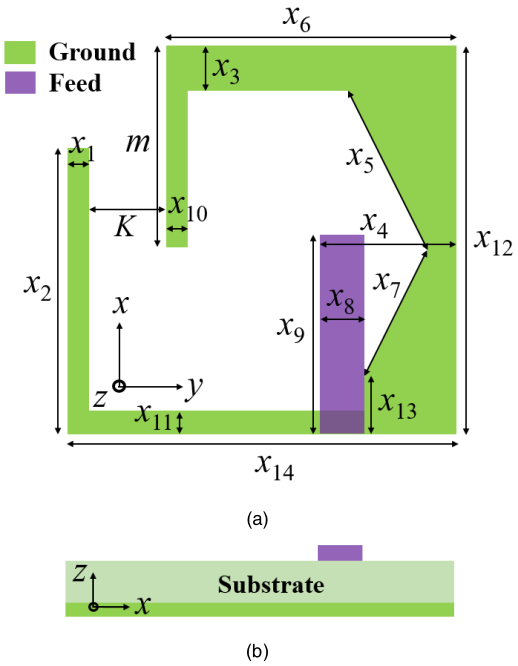

FIGURE 1. Schematic of the proposed unit cell: (a) top view, (b) side view.

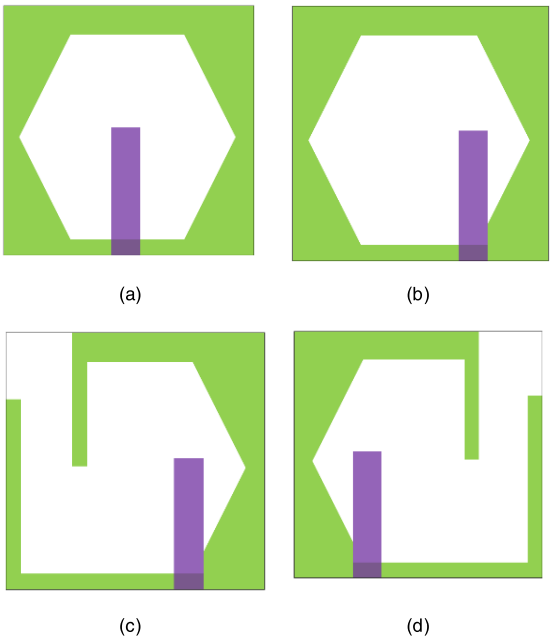

FIGURE 2. Evolution steps of the unit cell: (a) step-1, (b) step-2, (c) step-3 (proposed unit cell), (d) step-4 (mirror image of the proposed unit cell).

TABLE 1. Design parameters of the proposed antenna.

Parameter	Value (mm)	Parameter	Value (mm)
x_1, x_2, m, m_1, m_2, x_{10}, K	variable	d, e, f, g	variable
x_3	2.1	x_9	14
x_4	8.5	x_{11}	1
x_5	12	x_{12}	25
x_6	20.5	x_{13}	3.8
x_7	10	x_{14}	25
x_8	3	B	60

$$\varepsilon_{r_{eff}} = \frac{\varepsilon_r + 1}{2} \tag{2}$$

$$\Delta L = 0.412h\frac{\left(\varepsilon_{r_{eff}} + 0.3\right)\left(\frac{w}{h} + 0.264\right)}{\left(\varepsilon_{r_{eff}} - 0.258\right)\left(\frac{w}{h} + 0.8\right)} \tag{3}$$

where c is the speed of light in vacuum, x_5 is the aperture radius of the wide hexagonal slot, ε_r is the dielectric constant of the substrate, ΔL is the amount of length correction, w is the width of the radiator, and h is the height of the substrate.

The aperture radius (equal to x_5) of the wide slot affects the current path, which changes the resonating frequency band of the antenna. It can be seen from Fig. 3(a) that the unit cell in step-1 resonates ($S_{11} \leq -10$ dB) for 12.55–14.18 GHz band, and its polarization is LP.

In Fig. 2(b), the feed location of the antenna element is shifted towards the right side to increase its electrical length to obtain lower frequency bands. It can be seen from Figs. 3(b) and (c) that the unit cell in design step-2 resonates at 3.4–6.4 GHz frequency band, and its polarization is also LP.

Further, in Fig. 2(c), some portion of the metallic ground plane is etched out to form an open slot, and two arms facing towards each other are integrated for obtaining the CP band (the proposed unit cell). The two modes of E-field vectors with almost equal amplitude and 90° phase difference are excited by these two arms. It can be seen from Figs. 3(c) and (d) that the proposed unit cell resonates at 3.2–7.86 GHz frequency band with 3-dB ARBW of around 250 MHz (3.56–3.8 GHz with $m = 14.7$ mm, 3.45–3.7 GHz with $m = 16.2$ mm, 3.26–3.51 GHz with $m = 19.7$ mm). In all these cases, x_2 is assumed as 18 mm. Furthermore, it can be noticed from Table 2 that the unit cell retains its CP characteristics even after varying x_2, m, x_1, x_{10}, and K. The ARBW of the proposed unit cell can be easily changed by changing the arm length (m) of the CP radiator as illustrated in Fig. 3(d). In step-4, a mirror image of the proposed unit cell is presented (Fig. 2(d)), and its S_{11} and ARBW are shown in Figs. 3(b) and (c), respectively. It is to be noted that the responses of the proposed unit cell and its mirror image are nearly similar due to their identical shapes with opposite polarization senses.

The 3-dB AR beamwidth analysis of the proposed unit cell (step-3) is presented in Table 2. It is noticed that the maximum 3-dB AR beamwidths of 92.9° and 82.7° are obtained at 3.8 GHz (case-2) in the xz ($\varphi = 0°$) and yz ($\varphi = 90°$) planes, respectively. Correspondingly, in case-3, the maximum 3-dB AR beamwidths of 101.6° and 118.8° are obtained at 3.6 GHz in the xz- and yz-planes. Fig. 4 presents the 3-dB AR beamwidth of the proposed unit cell at 3.8 GHz.

It can be seen from the radiation patterns of Figs. 5(a) and (b) that the proposed unit cell radiates RHCP waves in $+z$-direction while its mirror image radiates LHCP waves in $+z$-direction. It can be further verified from the surface current distributions shown in Figs. 6 and 7 that the proposed unit cell and its mirror image radiate

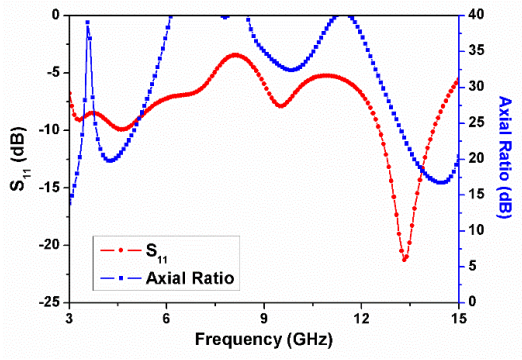

(a)

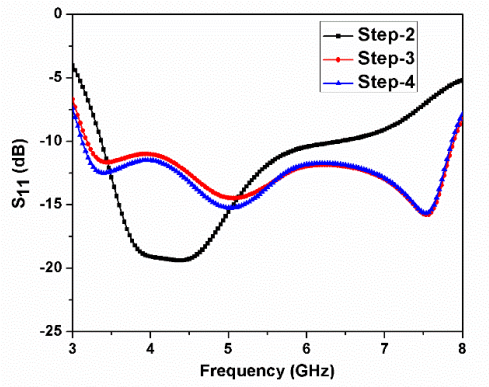

(b)

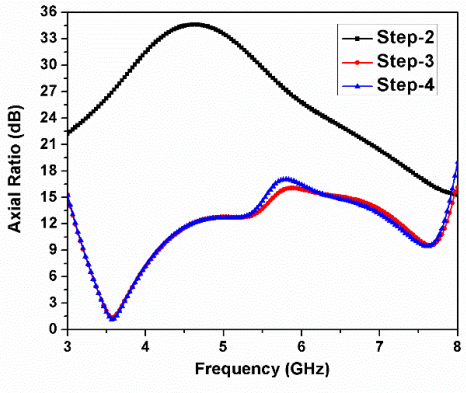

(c)

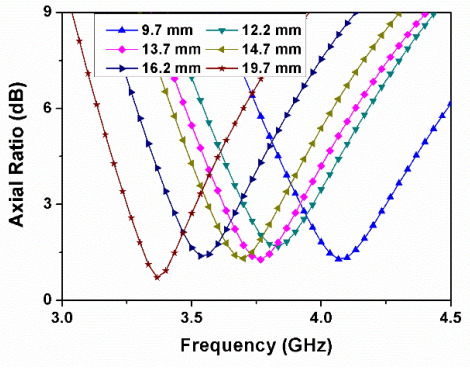

(d)

FIGURE 3. Simulated S_{11} and AR of the design steps: (a) step-1, (b) S_{11} of steps-2, −3, and −4, (c) AR of steps-2, −3, and −4, (d) AR variation with '*m*' in the proposed unit cell.

TABLE 2. Various cases of the proposed unit cell considered for ARBW and AR beamwidth analysis.

Case	x_2	m	x_1=x_{10}	K	3-dB ARBW (GHz)	3-dB AR Beamwidth (φ=0°)	3-dB AR Beamwidth (φ=90°)
1	18	15.7	1	3.5	3.48–3.73	95.9° (θ: -45.4° to 50.5°) (f=3.6 GHz)	111.7° (θ: -78.5° to 33.2°) (f=3.6 GHz)
2	18	15.7	3	1.5	3.53–3.8	92.9° (θ: -44.4° to 48.5°) (f=3.8 GHz)	81.7° (θ: -33.2° to 48.5°) (f=3.8 GHz)
3	17	15.7	1	3.5	3.45–3.72	101.6° (θ: -47° to 54.6°) (f=3.6 GHz)	118.8° (θ: -82° to 36.8°) (f=3.6 GHz)
4	17	15.7	3	1.5	3.54–3.8	98° (θ: -47° to 51°) (f=3.8 GHz)	80.3° (θ: -34.3° to 46°) (f=3.8 GHz)

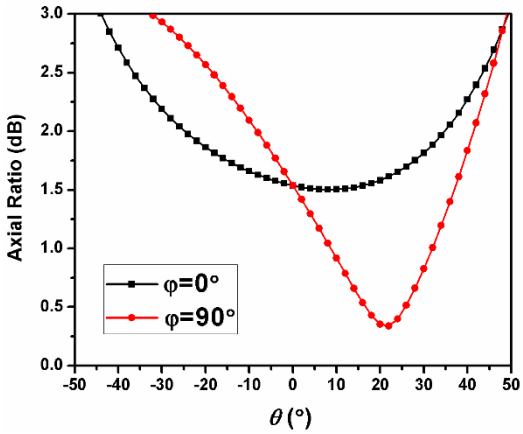

FIGURE 4. 3-dB AR beamwidth of the proposed unit cell at 3.8 GHz (case-2).

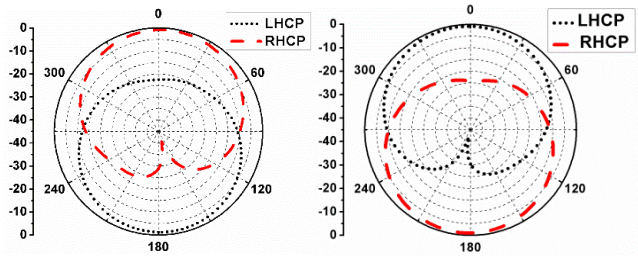

(a) (b)

FIGURE 5. Simulated radiation patterns at 3.6 GHz: (a) proposed unit cell, (b) mirror image of the proposed unit cell.

RHCP and LHCP waves, respectively. The dominant current vectors in Fig. 6 rotates counter-clockwise, which verifies the RHCP operation of the unit cell. On the other hand, in Fig. 7, the dominant current vectors in unit cell mirror image rotates clockwise, hence validating the LHCP operation.

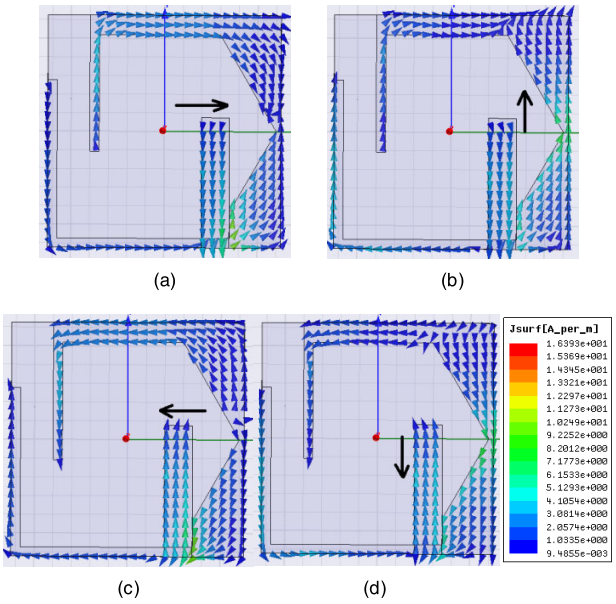

FIGURE 6. Surface current distribution in the proposed unit cell at 3.6 GHz (a) $\omega t = 0°$, (b) $\omega t = 90°$, (c) $\omega t = 180°$, (d) $\omega t = 270°$.

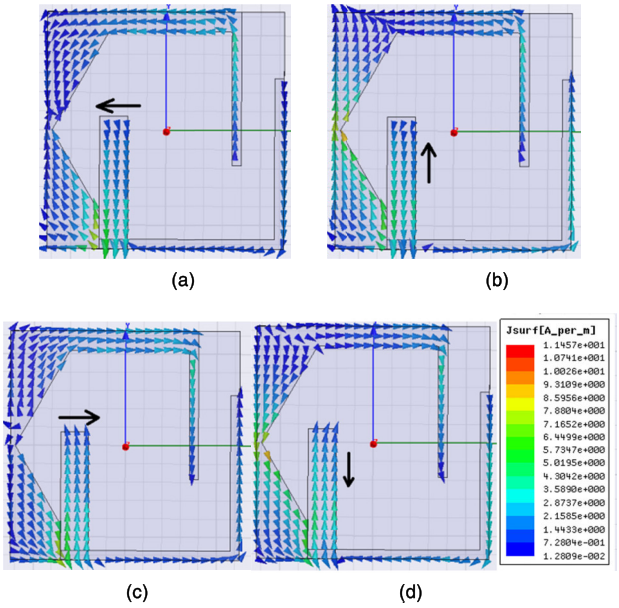

FIGURE 7. Surface current distribution in the mirror image of the proposed unit cell at 3.6 GHz (a) $\omega t = 0°$, (b) $\omega t = 90°$, (c) $\omega t = 180°$, (d) $\omega t = 270°$.

B. DESIGN OF FOUR-PORT DUAL CIRCULARLY-POLARIZED MIMO ANTENNA

The dual-CP MIMO antenna configurations (Config.-A and Config.-B) designed with the help of the proposed unit cell and its mirror image are shown in Fig. 8. In both antennas, the four-unit cells are positioned at the corners of the square-shaped substrate. The unit cells are placed so that the diagonally facing elements radiate the same type of waves. The inter-element spacing is $0.12\lambda_0$ (for $f_c = 3.6$ GHz) between the MIMO radiating elements for retaining 3-dB ARBW of the unit cells. In MIMO Config.-A, the arm length (m) of

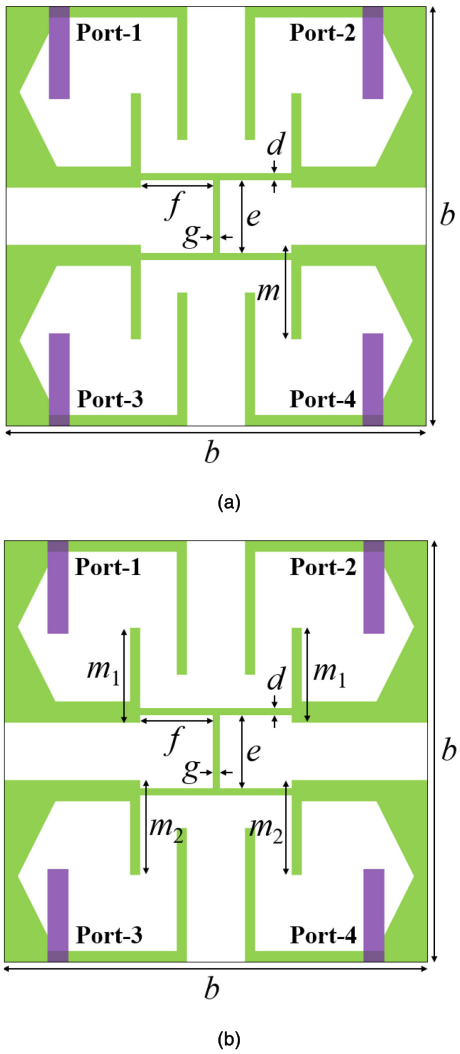

FIGURE 8. Layout of the proposed MIMO antenna: (a) Config.-A, (b) Config.-B.

the CP radiator is kept same for all the unit cells. On the other hand, in MIMO Config.-B, the CP radiator arm length is chosen as m_1 for antenna elements-1/-2 and as m_2 for antenna elements-3/-4. The design parameters of the MIMO antenna configurations are shown in Table 1.

It is important to note that the MIMO antenna cannot be used in practical applications if the ground planes of the unit cells are not connected, leading to undetermined reference voltages [20]. Keeping this in mind, in both configurations, the ground planes of the unit cells are connected using a metallic strip to provide a common reference plane for practical applications. An I-shaped metallic strip is used for connecting the ground planes of unit cells without disturbing the radiation characteristics of the unit cells. This step ensures an equal reference voltage level in both four-port MIMO configurations, thus making it integrable with other MMICs. In Section IV, it is also shown that the I-shaped strip helps in improving the 3-dB AR beamwidth of the MIMO Config.-B antenna.

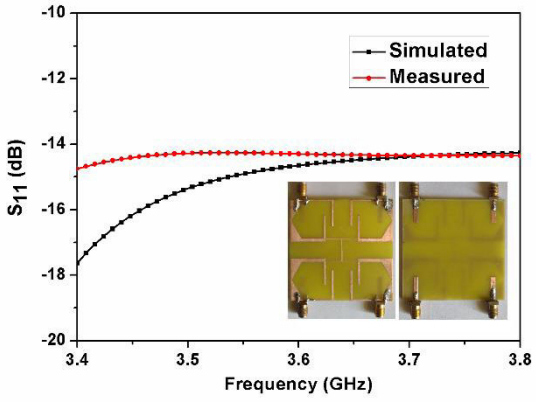

(a)

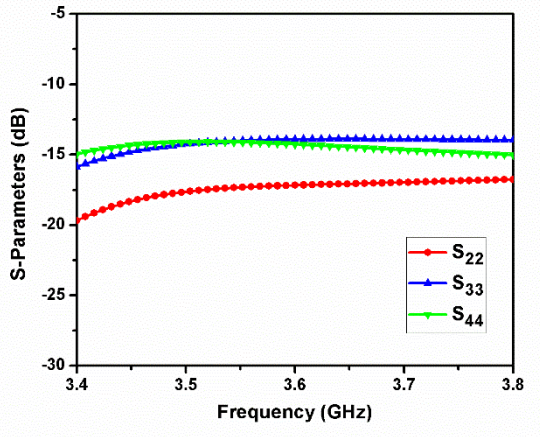

(b)

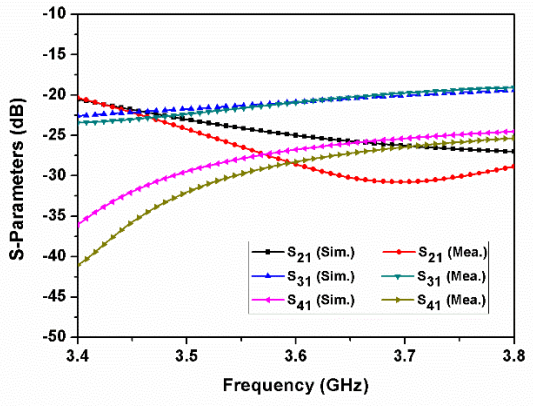

(c)

FIGURE 9. Simulated and measured results of the proposed MIMO antenna (Config.-A): (a) S_{11}, (b) simulated reflection coefficients, (c) S_{21}, S_{31}, and S_{41}.

III. RESULTS AND DISCUSSION

The results of the MIMO antenna configurations (Config.-A and Config.-B) are discussed in this section. The MIMO Config.-A (g=d=0.5 mm, m=15.7 mm, f=8.5 mm, and e=12.8 mm) prototype antenna is fabricated on the FR-4 substrate with dimension of $60\times60\times1.6$ mm^3 as shown in Fig. 9(a). The proposed MIMO Config.-A antenna is

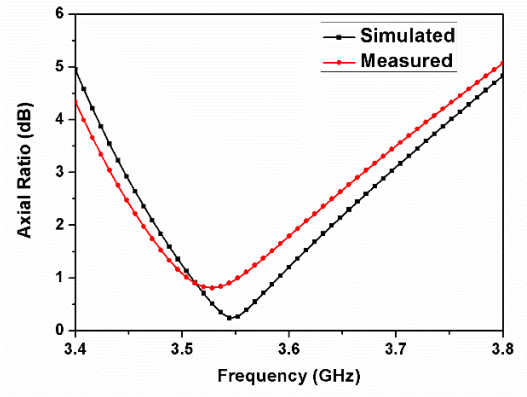

(a)

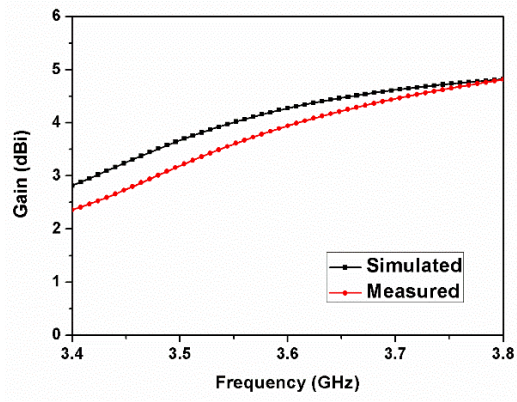

(b)

FIGURE 10. Proposed MIMO antenna (Config.-A) performance parameters (when port-1 is excited): (a) AR, (b) gain.

measured using the Anritsu MS2038C vector network analyzer and the Rohde & Schwarz FSP spectrum analyzer. The gain and AR of the fabricated antenna are measured inside an anechoic chamber using the method given in [24].

A. FABRICATED MIMO ANTENNA (CONFIG.-A)

It can be seen from Fig. 9(a) that the MIMO Config.-A antenna shows good impedance matching in the operating band of 3.4–3.8 GHz. The simulated reflection coefficients of the resonating element-2, -3, and -4 are shown in Fig. 9(b). It is also seen from Fig. 9(c) that the measured isolation is $>$20 dB between ports-1 and -2, $>$19 dB between ports-1 and -3, and $>$24 dB between ports-1 and -4.

The ARBW of the MIMO Config.-A antenna is shown in Fig. 10(a), and Table 3 presents different 3-dB ARBW cases (case-A to -G, when x_2 = 18 mm) of the antenna. It is noticed that the MIMO antenna exhibit 3-dB ARBW of $\sim$240 MHz (3.46–3.7 GHz). Furthermore, it can be seen from Table 3 that the MIMO Config.-A antenna exhibits circular polarization even when the parameters (g, d, e, and f) of the I-shaped element are varied. Therefore, flexibility is noticed in the design parameters of the I-shaped strip. The effect of varying arm length (m) on 3-dB ARBW of the MIMO antenna is shown in Fig. 11. The antenna exhibits 3-dB ARBW

TABLE 3. AR beamwidth of the MIMO Config.-A antenna with the I-shaped strip (when port-1 is excited).

Case	m	g, d	f	e	3-dB ARBW	3-dB AR beamwidth (φ=0°)	3-dB AR beamwidth (φ=90°)
A	15.7	0.5	9.25	12.8	3.42–3.65	85.4° (θ: -40.6° to 44.8°) (f=3.52 GHz)	56° (θ: -33.2° to 22.8°) (f=3.52 GHz)
B	16.5	0.5	9.25	12.8	3.4–3.62	69.64° (θ: -42.7° to 22.8°) (f=3.472 GHz)	59.6° (θ: -32.7° to 26.9°) (f=3.472 GHz)
C	16.5	1	9	12.8	3.4–3.58	94.8° (θ: -42.2° to 52.6°) (f=3.472 GHz)	50.7° (θ: -35.3° to 15.4°) (f=3.472 GHz)
D	16.5	2	8.5	12.8	3.4–3.58	61.8° (θ: -47.4° to 14.4°) (f=3.472 GHz)	49.78° (θ: -31.7° to 18.08°) (f=3.472 GHz)
E	16.5	3	8	12.8	3.4–3.59	61.78° (θ: -43.7° to 18.08°) (f=3.52 GHz)	52.32° (θ: -44.2° to 8.12°) (f=3.52 GHz)
F	16.5	4	7.5	12.8	3.44–3.6	117.8° (θ: -46.3° to 71.5°) (f=3.536 GHz)	38.24° (θ: -28.04° to 10.2°) (f=3.536 GHz)
G	15.7	0.5	9.25	14.8	3.43–3.66	108.6° (θ: -47.1° to 61.5°) (f=3.536 GHz	57.8° (θ: -35.3° to 22.5°) (f=3.536 GHz)

of 3.4–3.62 GHz with m = 16.2 mm, 3.46–3.7 GHz with m = 15.7 mm, and 3.59–3.8 GHz with m = 13.7 mm. Hence, by varying the arm length (m), the ARBW can be easily shifted in the proposed MIMO antenna. The 3-dB AR beamwidth analysis of the MIMO Config.-A antenna is discussed in the next section.

The simulated and measured gain plots of the MIMO Config.-A are shown in Fig. 10(b). It is found that the maximum gain of the antenna is around 4.5 dBi in the operating band.

The diversity performance of the MIMO antenna is evaluated by measuring the envelope correlation coefficient (ECC) between ports-1 and -2, ports-1 and -3, and ports-1 and -4. In the proposed work, the ECC is calculated by using far-field relation [25]

$$\rho_e = \frac{\left|\int\int\left[\vec{F}_1(\theta,\varphi)\,\vec{F}_2(\theta,\varphi)\right]d\Omega\right|^2}{\int\int\left|\vec{F}_1(\theta,\varphi)\right|^2 d\Omega \int\int\left|\vec{F}_2(\theta,\varphi)\right|^2 d\Omega} \quad (4)$$

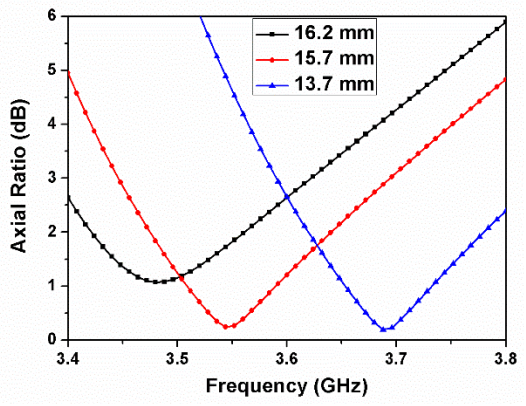

FIGURE 11. Operating band variation with arm length (m) for the proposed MIMO antenna (Config.-A) (when port-1 is excited).

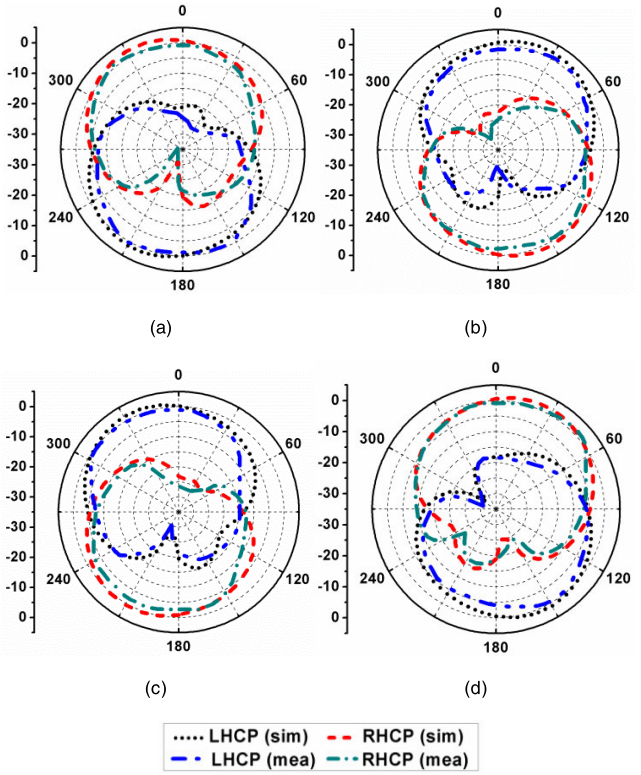

FIGURE 12. Radiation patterns at 3.6 GHz (Config.-A) when (a) port-1 is excited, (b) port-2 is excited, (c) port-3 is excited, (d) port-4 is excited.

where F is the radiated field, Ω, θ, and φ are the solid, elevation, and azimuthal angles, respectively. It is found that ECC is less than 0.12 between various antenna ports, which verifies the diversity performance of the proposed MIMO antenna.

The diversity gain (DG) between different ports of the MIMO antenna is found to be around 10 dB in the band of interest. The radiation patterns of the proposed MIMO antenna at 3.6 GHz are shown in Fig. 12. The antenna displays dual circular polarization characteristics by radiating RHCP waves when port-1/-4 is excited, and LHCP waves when

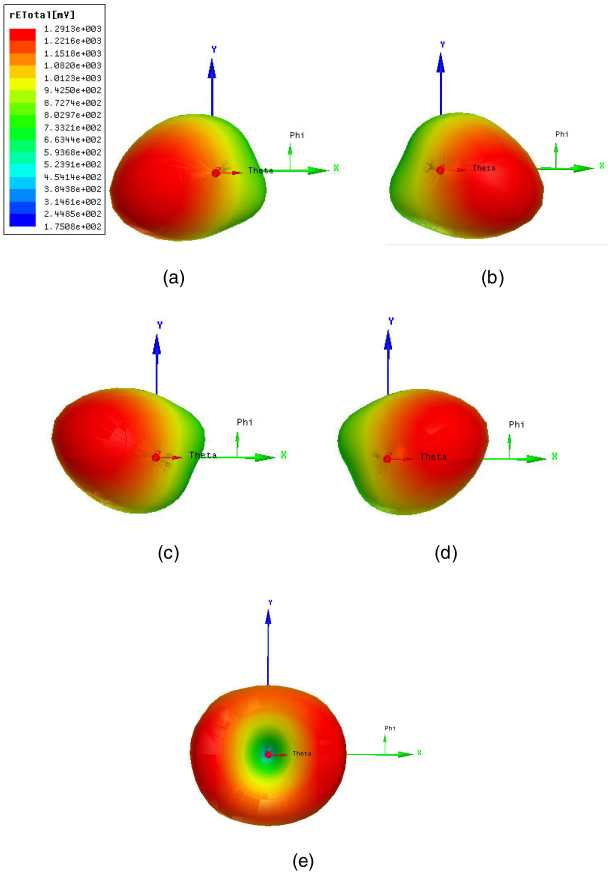

FIGURE 13. 3-D radiation patterns of the MIMO Config.-A antenna at 3.6 GHz when (a) port-1 is excited, (b) port-2 is excited, (c) port-3 is excited, (d) port-4 is excited, (e) all ports are excited.

port-2/-3 is excited. Fig. 13 shows 3-D radiation patterns of the antenna at 3.6 GHz.

B. PROPOSED MIMO ANTENNA (CONFIG.-B)

As discussed in the previous section, the proposed MIMO Config.-A antenna has 3-dB ARBW of around 240 MHz in the band of interest (3.4–3.8 GHz). It is also shown that its CP band can be easily shifted by varying m. The MIMO Config.-B antenna covers the entire 3.4–3.8 GHz band by making some alterations in the CP radiator arm length. As shown in Fig. 8(b), the arm length of the antenna elements-1 and -2 is m_1, while the arm length of the antenna elements-3 and -4 is m_2. The optimized values of m_1 and m_2 are chosen as 16.5 mm and 12.7 mm, respectively (with f=9.25 mm, x_2=18 mm, e=12.8 mm, g=d=0.5 mm). Similarly, other values of m_1 (like 15.7 mm) can also be considered as illustrated in Table 3.

The impedance bandwidth, isolation, ECC, and gain of the MIMO Config.-B antenna are almost similar to the MIMO Config.-A antenna. Therefore, only the 3-dB ARBW and LHCP/RHCP radiation patterns of the MIMO Config.-B antenna are shown here. It can be easily seen from Figs. 14 and 15 that the port-1 radiates RHCP waves and the port-2 radiates LHCP waves with 3-dB ARBW

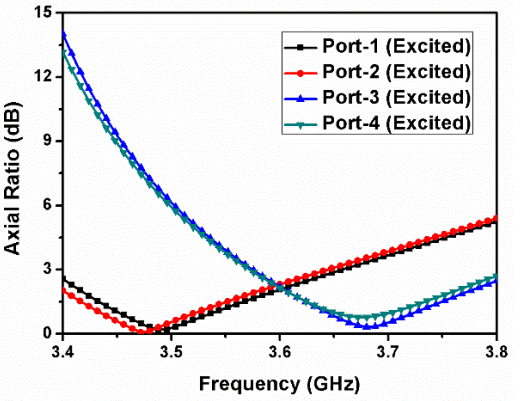

FIGURE 14. Proposed MIMO Config.-B AR performance (when different ports are excited).

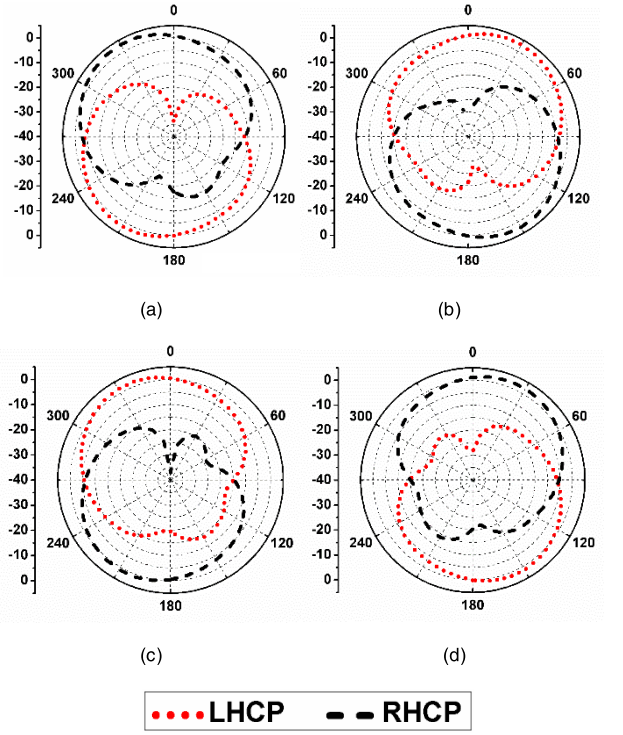

FIGURE 15. Radiation patterns of the proposed MIMO Config.-B antenna when (a) port-1 is excited (3.48 GHz), (b) port-2 is excited (3.48 GHz), (c) port-3 is excited (3.68 GHz), (d) port-4 is excited (3.68 GHz).

of 3.4–3.65 GHz. On the other hand, the port-3 radiates LHCP waves and the port-4 radiates RHCP waves with 3-dB ARBW of 3.57–3.8 GHz. Therefore, the Config.-B antenna covers the entire 3.4–3.8 GHz bandwidth, and also offers choice in polarizations (LHCP/RHCP). The 3-dB AR beamwidth performance of the MIMO Config.-A and Config.-B (with/without I-shaped strip) antennas is discussed in detail in the next section.

IV. BEAMWIDTH ANALYSIS OF THE PROPOSED MIMO ANTENNA

In this section, the 3-dB AR beamwidth performance of the MIMO Config.-A/-B (with/without I-shaped strip) antennas is analyzed.

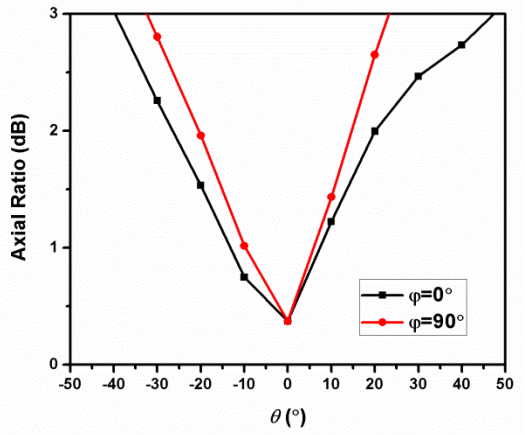

(a)

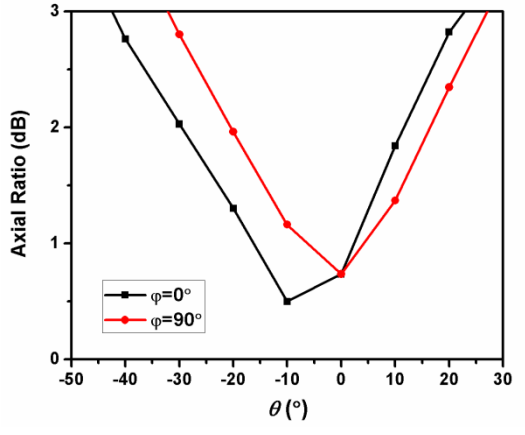

(b)

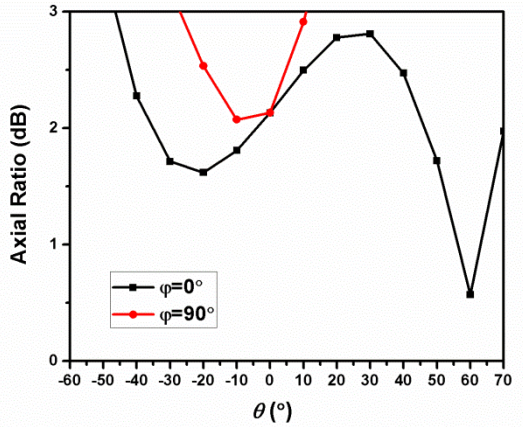

(c)

FIGURE 16. 3-dB AR beamwidth of the MIMO Config.-A: (a) case-A at 3.52 GHz, (b) case-B at 3.472 GHz, (c) case-F at 3.536 GHz.

A. 3-dB AR BEAMWIDTH PERFORMANCE OF THE MIMO CONFIG.-A ANTENNA

Various cases (case-A to -G) of the 3-dB AR beamwidth are considered to study the effect of the I-shaped strip parameters (*g*, *d*, and *e*). During the study, only I-shaped strip parameters are varied, and the CP radiator arm length x_2 is kept fixed at 18 mm. The CP radiator arm length (*m*) is changed from 15.7 mm to 16.5 mm to illustrate that the antenna can achieve desirable AR performance even with a change in *m*. It is seen from Fig. 16 and Table 3 that the proposed MIMO antenna offers satisfactory 3-dB AR beamwidth performance in the *xz*-plane for all cases (except case-B and case-E). On the other hand, the 3-dB AR beamwidth is not satisfactory in the *yz*-plane (for all cases considered). Table 3 displays all the cases of the MIMO Config.-A antenna, and it is seen that the maximum 3-dB AR beamwidth of 117.8° (θ: −46.3° to 71.5°) is obtained in the *xz*-plane at 3.536 GHz (for case-F). On the other hand, for case-F, the 3-dB AR beamwidth of 38.24° is obtained in the *yz*-plane (θ: −28.04° to 10.2°) at 3.536 GHz. Therefore, it can be said that, after observing Table 3 and Fig. 16, the beamwidth performance of the Config.-A antenna is not satisfactory in the *yz*-plane.

TABLE 4. AR beamwidth of the MIMO Config.-B with I-shaped strip (m_2 = 12.7 mm) (port-1 is excited).

Case	m_1	*g*, *d*	*f*	*e*	3-dB ARBW	3-dB AR beamwidth (φ=0°)	3-dB AR beamwidth (φ=90°)
A	15.7	0.5	9.25	12.8	3.45–3.71	80.1° (θ: -45.3° to 34.8°) (*f*=3.504 GHz)	79.1° (θ: -41.1° to 38°) (*f*=3.504 GHz)
B	16.5	0.5	9.25	12.8	3.4–3.66	80.3° (θ: -40.3° to 40°) (*f*=3.472 GHz)	77° (θ: -42° to 35°) (*f*=3.472 GHz)
C	16.5	1	9	12.8	3.41–3.7	107.6° (θ: -48.8° to 58.8°) (*f*=3.472 GHz)	86.2° (θ: -45.6° to 40.6°) (*f*=3.472 GHz)
D	16.5	2	8.5	12.8	3.43–3.72	113.17° (θ: -52.1° to 61.07°) (*f*=3.536 GHz)	90.6° (θ: -54.2° to 36.4°) (*f*=3.536 GHz)
E	16.5	3	8	12.8	3.48–3.72	108.4° (θ: -52.6° to 55.8°) (*f*=3.52 GHz)	82.7° (θ: -43.2° to 39.5°) (*f*=3.52 GHz)
F	16.5	4	7.5	12.8	3.48–3.74	118.9° (θ: -52.1° to 66.8°) (*f*=3.536 GHz)	92.7° (θ: -45.8° to 46.9°) (*f*=3.536 GHz)
G	15.7	0.5	9.25	14.8	3.51–3.75	100° (θ: -44.9° to 55.1°) (*f*=3.576 GHz)	79.2° (θ: -48° to 31.2°) (*f*=3.576 GHz)

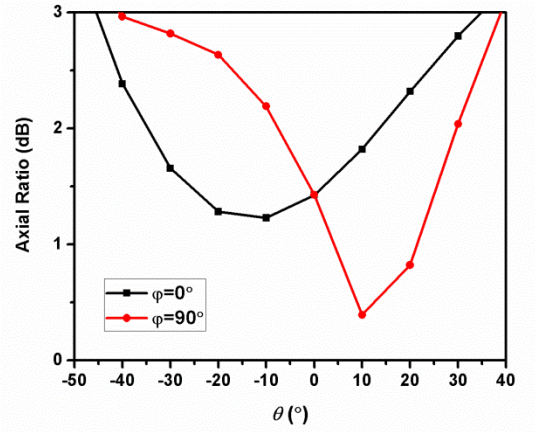

(a)

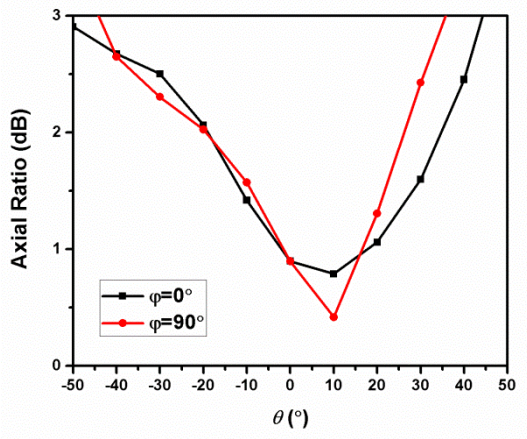

(b)

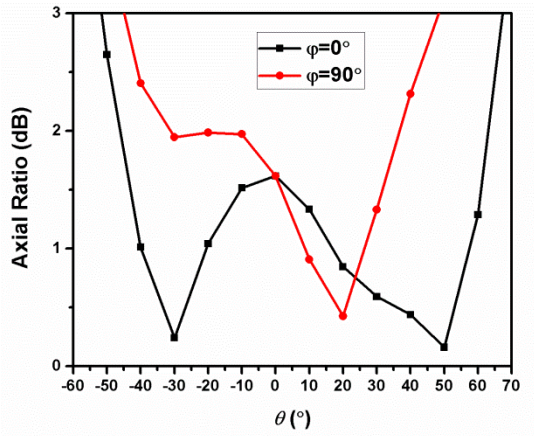

(c)

FIGURE 17. 3-dB AR beamwidth of the MIMO Config.-B antenna (m_2 = 12.7 mm): (a) case-A at 3.504 GHz, (b) case-B at 3.472 GHz, (c) case-F at 3.536 GHz.

B. 3-dB AR BEAMWIDTH PERFORMANCE OF THE MIMO CONFIG.-B ANTENNA

Various cases (case-A to case-G) of the 3-dB AR beamwidth are considered for analysis of the MIMO Config.-B antenna. Table 4 shows different cases with m_1 = 16.5 mm/m_2 = 12.7 mm and m_1 = 15.7 mm/m_2 = 12.7 mm. It is seen from Fig. 17 and Table 4 that the MIMO antenna has satisfactory 3-dB AR beamwidth performance in both *xz*-and *yz*-planes (for all the cases). It is seen from Fig. 17(c) that the maximum 3-dB AR beamwidths of 118.9° (θ: −52.1° to 66.8°) and 92.7° (θ: −45.8° to 46.9°) are obtained in the *xz*- and *yz*-planes, respectively, at 3.536 GHz in the case-F. Therefore, after observing the results, it can be concluded that the MIMO Config.-B antenna outperforms the MIMO Config.-A antenna in terms of the 3-dB AR beamwidth in both *xz*- and *yz*-planes.

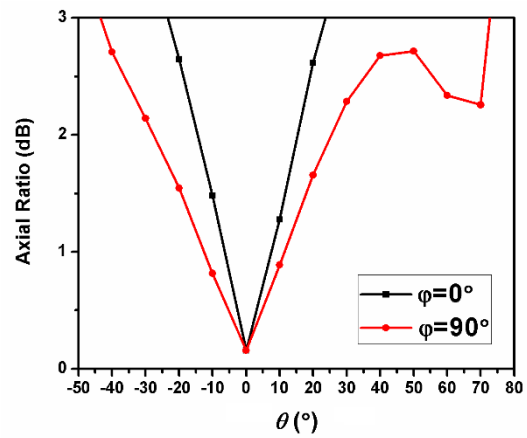

(a)

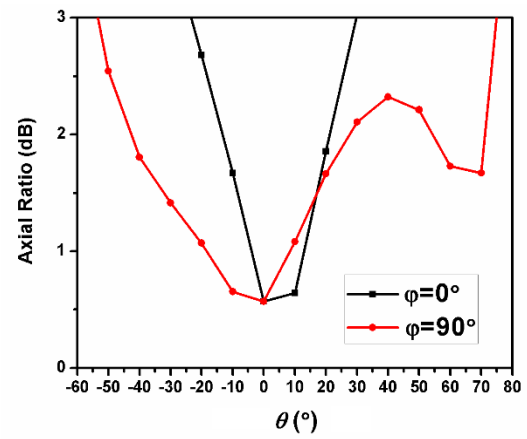

(b)

FIGURE 18. 3-dB AR beamwidth of the MIMO Config.-B antenna (without the I-shaped strip) at 3.44 GHz: (a) m_1 = 15.7 mm, m_2 = 12.7 mm, (b) m_1 = 16.5 mm, m_2 = 12.7 mm.

The use of two different arm lengths (m_1 and m_2) for unit cells at port-1/2 and port-3/4, respectively, with the I-shaped strip helps in adjusting the E-field magnitude of two modes radiated by the arms of the CP radiators. This modification keeps the AR beamwidth below 3-dB in both *xz*- and *yz*-planes with the Config.-B antenna.

Also, the power concentrated in the lower arm of the unit cell (when port-1 or port-2 is excited) gets redistributed in the I-shaped strip (which does not act as a radiator). It is also important to note that, if $m_1 > m_2$, the AR beamwidth will be

TABLE 5. AR beamwidth of the MIMO Config.-B antenna without the I-shaped strip (port-1 is excited).

Case	3-dB ARBW	3-dB AR beamwidth (φ=0°)	3-dB AR beamwidth (φ=90°)
m_1=15.7 mm, m_2=12.7 mm	3.4–3.61	47.6° (θ: -23.8° to 23.8°) (f=3.44 GHz)	114.9° (θ: -43° to 71.9°) (f=3.44 GHz)
m_1=16.5 mm, m_2=12.7 mm	3.4–3.61	51.2° (θ: -22.5° to 28.7°) (f=3.44 GHz)	128.6° (θ: -54.3° to 74.3°) (f=3.44 GHz)

achieved in the *xz*- and *yz*-planes if the port-1/-2 is excited. On the other hand, if $m_2 > m_1$, the same can be said for the port-3/-4. By varying m_1 and m_2, the 3-dB AR beamwidth can be easily obtained in both *xz*- and *yz*-planes for other frequency bands, too.

C. 3-dB AR BEAMWIDTH PERFORMANCE OF THE MIMO CONFIG.-B ANTENNA WITHOUT THE I-SHAPED STRIP

In this section, the effect of the I-shaped strip on the 3-dB AR beamwidth is explained. To understand its effect, the I-shaped strip is removed from the MIMO Config.-B antenna as shown in Figs. 18(a) and (b) and Table 5 (with $m_1 = 16.5$ mm/$m_2 = 12.7$ mm and $m_1 = 15.7$ mm/$m_2 = 12.7$ mm). In MIMO Config.-B without the I-shaped strip ($m_1 = 15.7$ mm/$m_2 = 12.7$ mm), the maximum 3-dB AR beamwidths of 47.6° (θ: −23.8° to 23.8°) and 114.9° (θ: −43° to 71.9°) are obtained in the *xz*- and *yz*-planes at 3.44 GHz, respectively. On the other hand, with $m_1 = 16.5$ mm and $m_2 = 12.7$ mm, the maximum 3-dB AR beamwidths of 51.2° (θ: −22.5° to 28.7°) and 128.6° (θ: −54.3° to 74.3°) are obtained in the *xz*- and *yz*-planes at 3.44 GHz, respectively. Therefore, it is noticed that the MIMO antenna without the I-shaped strip shows unsatisfactory 3-dB AR beamwidth performance in the *xz*-plane at 3.44 GHz. Contrary to this, the 3-dB AR beamwidth performance of the MIMO antenna without the I-shaped strip is satisfactory in the *yz*-plane at 3.44 GHz. The same holds at other frequencies, too, but here only the maximum achievable 3-dB beamwidth of the Config.-B (without I-shaped strip) antenna is shown. Therefore, it can be concluded from the above discussion:

- The proposed MIMO Config.-B antenna outperforms the MIMO Config.-A and Config.-B (without I-shaped strip) antennas in terms of the 3-dB AR beamwidth in both *xz*- both *xz*- and *yz*-planes.
- Only two ports can be utilized for the 3-dB AR beamwidth purpose (either port-1/-2 or port-3/-4) in Config.-B. If $m_1 > m_2$, the AR achieved in the *xz*- and *yz*-planes when the port-1/-2 is excited. On the other hand, if $m_2 > m_1$, the same can be said for the the port-3/-4.

TABLE 6. Comparison of the proposed MIMO antenna and other reported planar CP/dual-CP MIMO antennas.

Ref.	[14]	[16]	[17]	[18]	[19]	Prop.
No. of Ports	3	4	2	2	2	4
-10 dB Band (GHz)	5.5–6.25	1.71–1.88, 3.3–3.7, 5.12–5.37	5.49–6.024	3.5–8.2	2–4.76	3.4–3.8
IBW (GHz)	0.75	0.17, 0.4, 0.25	0.534	4.7	2.76	0.4
3-dB AR Band (GHz)	5.61–5.7	3.56–3.67, 5.16–5.29	5.772–5.864	4.6–7.6	2–3.7	Config.-A (3.46–3.7) (m=15.7 mm), Config.-B (3.4–3.65 at port-1/-2 and 3.57–3.8 GHz at port-3/-4)
ARBW (%)	12	27.5, 52	17	63.8	61.5	62.5
Peak Gain (dBi)	4.7	----	5.34	9.9	4	4.5
ECC	<0.01 (Far-field)	----	<0.15 (S-parameter)	< 0.0006 (S-parameter)	----	<0.12 (Far-field)
App.	WLAN	GSM, Wi-MAX, WLAN	BT, Wi-MAX	WLAN, Wi-MAX	UWB	Sub-6 GHz
Ant. Size (mm^2)	29×48	165×165	60×60	32×32	48×48	60×60
Feed	MS	MS	CPW	MS	CPW	MS
Iso. (dB)	>18	>37	>33	>15	>15	>19
CG	Yes	No	Yes	No	Yes	Yes
Dual-CP	No	No	Yes	Yes	Yes	Yes

IBW: Impedance bandwidth, AR: Axial ratio, BH: Beamwidth, App.: Application, Ant.: Antenna, Iso.: Isolation, CG: Connected ground, BT: Bluetooth, UWB: Ultra-wideband, MS: Microstrip

- The 3-dB AR beamwidth for other frequency bands can be easily obtained in Config.-B by taking suitable values of m_1 and m_2.
- The I-shaped strip plays a significant role in the MIMO antenna design since the 3-dB AR beamwidth performance of Config.-B deteriorates (in the *xz*-plane) if the strip is removed. Therefore, in addition to setting an equal voltage reference level in the ground plane, the I-shaped strip is also responsible for achieving the desirable 3-dB beamwidth in both *xz*- and *yz*-planes in Config.-B.

The comparison of the proposed MIMO antenna (Config.-A and Config.-B) with other reported planar CP/dual-CP MIMO antennas is presented in Table 6. The proposed MIMO antenna outperforms the other dual-CP four-port MIMO antennas reported in [17]–[19] in terms of isolation and the number of available ports. In addition,

the proposed MIMO antenna offers advantages of providing a connected ground plane, relatively small size, and dual circular polarization as compared with other four-port CP MIMO antennas reported in [14], [16].

V. CONCLUSION

Two configurations (Config.-A and Config.-B) of a four-port dual-CP MIMO antenna are presented. Both configurations show dual circular polarization by radiating RHCP waves when ports-1 and -4 are excited, and LHCP waves when ports-2 and -3 are excited. The MIMO Config.-A antenna can be used when there is a requirement of the same CP band from all the unit cells with polarization choice (LHCP/RHCP). On the other hand, the MIMO Config.-B antenna can be used to cover entire 3.4–3.8 GHz band (port-1/2 and port-3/4 radiating different CP bands) with LHCP/RHCP choice. The Config.-B antenna could also be suitable in applications where wide 3-dB AR beamwidth is required in both *xz*- and *yz*-planes. It is also shown that the I-shaped strip plays a crucial role in improving 3-dB AR beamwidth in addition to connecting the ground planes to obtain an equal reference voltage level. Wide 3-dB AR beamwidths of 118.9° and 92.7° are obtained at 3.536 GHz in the *xz*- and *yz*-planes, respectively, in case-F of the Config.-B antenna. The fabricated MIMO antenna prototype (Config.-A) achieves satisfactory diversity performance in terms of ECC, isolation, and diversity gain. The proposed MIMO antenna configurations are compact in size and can be easily integrated with portable MMICs due to planar geometry and a common ground surface. The MIMO antenna configurations presented in this work can be utilized for sub-6 GHz 5G applications.

REFERENCES

[1] V. C. Papamichael and P. Karadimas, "Performance evaluation of actual multielement antenna systems under transmit antenna Selection/Maximal ratio combining," *IEEE Antennas Wireless Propag. Lett.*, vol. 10, pp. 690–692, 2011.
[2] S. Saxena, B. K. Kanaujia, S. Dwari, S. Kumar, and R. Tiwari, "MIMO antenna with built-in circular shaped isolator for sub-6 GHz 5G applications," *Electron. Lett.*, vol. 54, no. 8, pp. 478–480, Apr. 2018.
[3] Y. Ou, X. Cai, and K. Qian, "Two-element compact antennas decoupled with a simple neutralization line," *Prog. Electromagn. Res. Lett.*, vol. 65, pp. 63–68, 2017.
[4] S. Saxena, B. K. Kanaujia, S. Dwari, S. Kumar, and R. Tiwari, "A compact dual-polarized MIMO antenna with distinct diversity performance for UWB applications," *IEEE Antennas Wireless Propag. Lett.*, vol. 16, pp. 3096–3099, 2017.
[5] M. Bilal, R. Saleem, H. H. Abbasi, M. F. Shafique, and A. K. Brown, "An FSS-based nonplanar quad-element UWB-MIMO antenna system," *IEEE Antennas Wireless Propag. Lett.*, vol. 16, pp. 987–990, 2017.
[6] M. G. N. Alsath, H. Arun, Y. P. Selvam, M. Kanagasabai, S. Kingsly, S. Subbaraj, R. Sivasamy, S. K. Palaniswamy, and R. Natarajan, "An integrated tri-band/UWB polarization diversity antenna for vehicular networks," *IEEE Trans. Veh. Technol.*, vol. 67, no. 7, pp. 5613–5620, Jul. 2018.
[7] S. K. Palaniswamy, Y. P. Selvam, M. G. N. Alsath, M. Kanagasabai, S. Kingsly, and S. Subbaraj, "3-D eight-port ultrawideband antenna array for diversity applications," *IEEE Antennas Wireless Propag. Lett.*, vol. 16, pp. 569–572, 2017.
[8] J. Zhu, S. Li, B. Feng, L. Deng, and S. Yin, "Compact dual-polarized UWB quasi-self-complementary MIMO/diversity antenna with band-rejection capability," *IEEE Antennas Wireless Propag. Lett.*, vol. 15, pp. 905–908, 2016.
[9] S. Saxena, B. K. Kanaujia, S. Dwari, S. Kumar, and R. Tiwari, "Compact microstrip antennas with very wide ARBW and triple circularly polarized bands," *Int. J. RF Microw. Comput.-Aided Eng.*, vol. 28, no. 1, Jan. 2018, Art. no. e21162.
[10] S. Kumar, K. W. Kim, H. C. Choi, S. Saxena, R. Tiwari, M. K. Khandelwal, S. K. Palaniswamy, and B. K. Kanaujia, "A low profile circularly polarized UWB antenna with integrated GSM band for wireless communication," *AEU Int. J. Electron. Commun.*, vol. 93, pp. 224–232, Sep. 2018.
[11] F. A. Dicandia, S. Genovesi, and A. Monorchio, "Analysis of the performance enhancement of MIMO systems employing circular polarization," *IEEE Trans. Antennas Propag.*, vol. 65, no. 9, pp. 4824–4835, Sep. 2017.
[12] J. Wang, Z. Lv, and X. Li, "Analysis of MIMO diversity improvement using circular polarized antenna," *Int. J. Antennas Propag.*, vol. 2014, Feb. 2014, Art. no. 570923.
[13] J. Malik, A. Patnaik, and M. V. Kartikeyan, "Novel printed MIMO antenna with pattern and polarization diversity," *IEEE Antennas Wireless Propag. Lett.*, vol. 14, pp. 739–742, 2015.
[14] Y. Sharma, D. Sarkar, K. Saurav, and K. V. Srivastava, "Three-element MIMO antenna system with pattern and polarization diversity for WLAN applications," *IEEE Antennas Wireless Propag. Lett.*, vol. 16, pp. 1163–1166, 2017.
[15] M. Akbari, H. Abo Ghalyon, M. Farahani, A.-R. Sebak, and T. A. Denidni, "Spatially decoupling of CP antennas based on FSS for 30-GHz MIMO systems," *IEEE Access*, vol. 5, pp. 6527–6537, 2017.
[16] R. S. Parbat, A. R. Tambe, M. B. Kadu, and R. P. Labade, "Dual polarized triple band 4×4 MIMO antenna with novel mutual coupling reduction approach," in *Proc. IEEE Bombay Sect. Symp. (IBSS)*, Sep. 2015, pp. 1–6.
[17] L. Malviya, R. K. Panigrahi, and M. V. Kartikeyan, "Circularly polarized 2×2 MIMO antenna for WLAN applications," *Prog. Electromagn. Res. C*, vol. 66, pp. 97–107, 2016.
[18] M. Jalali, M. Naser-Moghadasi, and R. A. Sadeghzadeh, "Dual circularly polarized multilayer MIMO antenna array with an enhanced SR-feeding network for C-band application," *Int. J. Microw. Wireless Technol.*, vol. 9, no. 8, pp. 1741–1748, Oct. 2017.
[19] R. Kumar Saini and S. Dwari, "A broadband dual circularly polarized square slot antenna," *IEEE Trans. Antennas Propag.*, vol. 64, no. 1, pp. 290–294, Jan. 2016.
[20] C. D. S. and S. S. Karthikeyan, "A novel broadband dual circularly polarized microstrip-fed monopole antenna," *IEEE Trans. Antennas Propag.*, vol. 65, no. 3, pp. 1410–1415, Mar. 2017.
[21] Z. Li, X. Zhu, and C. Yin, "CPW-fed ultra-wideband slot antenna with broadband dual circular polarization," *AEU - Int. J. Electron. Commun.*, vol. 98, pp. 191–198, Jan. 2019.
[22] M. S. Sharawi, "Current misuses and future prospects for printed multiple-input, multiple-output antenna systems [Wireless Corner]," *IEEE Antennas Propag. Mag.*, vol. 59, no. 2, pp. 162–170, Apr. 2017.
[23] C. A. Balanis, *Antenna Theory: Analysis and Design*. Hoboken, NJ, USA: Wiley, 2005.
[24] B. Yen Toh, R. Cahill, and V. F. Fusco, "Understanding and measuring circular polarization," *IEEE Trans. Educ.*, vol. 46, no. 3, pp. 313–318, Aug. 2003.
[25] S. Blanch, J. Romeu, and I. Corbella, "Exact representation of antenna system diversity performance from input parameter description," *Electron. Lett.*, vol. 39, no. 9, p. 705, 2003.

SHOBHIT SAXENA received the B.Tech. degree in electronics and communication engineering and the M.Tech. degree in digital communication, in 2005 and 2010, respectively. He is currently pursuing the Ph.D. degree in microwave engineering with IIT (ISM), Dhanbad, India. He had worked as a Research Scholar with Tohoku University, Japan, from 2006 to 2008. His current research interests include wideband microstrip antennas, ultra-wideband antennas, circularly-polarized antennas, and microwave components. He was a recipient of the Japanese Government (Monbukagakusho: MEXT) Scholarship.

BINOD KUMAR KANAUJIA received the B.Tech. degree in electronics engineering from the Kamla Nehru Institute of Technology, Sultanpur, India, in 1994, and the M.Tech. and Ph.D. degrees from the Department of Electronics Engineering, IIT Banaras Hindu University, Varanasi, India, in 1998 and 2004, respectively. He is currently a Professor with the School of Computational and Integrative Sciences, Jawaharlal Nehru University, New Delhi, India. He has been credited to publish more than 250 research articles with more than 1900 citations and H-index of 21 in several peer-reviewed journals and conferences. He had supervised 50 M.Tech. and 15 Ph.D. scholars in the field of RF and microwave engineering. He is also a member of several academic and professional bodies, such as the Institution of Engineers, India, the Indian Society for Technical Education, and the Institute of Electronics and Telecommunication Engineers of India. He had successfully executed five research projects sponsored by several agencies of the Government of India, such as DRDO, DST, AICTE, and ISRO. He is currently on the editorial board of several international journals.

SANTANU DWARI received the B.Tech. and M.Tech. degrees in radio physics and electronics from the University of Calcutta, West Bengal, India, in 2000 and 2002, respectively, and the Ph.D. degree from IIT Kharagpur, India, in 2009. In 2008, he joined the Department of Electronics Engineering, IIT (ISM), Dhanbad, India, as an Assistant Professor. He has published more than 100 research articles in refereed international journals/conferences. His current research interests include computational electromagnetics, antennas, and RF planar circuits. He is carrying out two sponsored research project as a Principal Investigator.

SACHIN KUMAR received the B.Tech. degree in electronics and communication engineering from Uttar Pradesh Technical University, Lucknow, India, in 2009, and the M.Tech. and Ph.D. degrees in electronics and communication engineering from Guru Gobind Singh Indraprastha University, India, in 2011 and 2016, respectively. He is currently a Postdoctoral Researcher with the School of Electronics Engineering, Kyungpook National University, Daegu, South Korea. His current research interests include circularly-polarized microstrip antennas, reconfigurable antennas, ultra-wideband antennas, defected ground structure, and microwave components.

HYUN CHUL CHOI received the B.S. degree in electronics engineering from Kyungpook National University, Daegu, South Korea, in 1982, and the M.S. and Ph.D. degrees in electronics engineering from the Korea Advanced Institute of Science and Technology (KAIST), South Korea, in 1984 and 1989, respectively. In 1990, he joined Kyungpook National University, as a Professor, where he has been serving as the Dean of the IT College. He has published numerous articles in the fields of EMI/EMC, scattering and propagation station, and RF/microwave circuits and systems.

KANG WOOK KIM received the B.S. and M.S. degrees in electrical engineering from Seoul National University, South Korea, in 1985 and 1987, respectively, and the Ph.D. degree in electrical engineering from the University of California at Los Angeles, USA, in 1996. In 1987, he was a Researcher with the Korea Electrotechnology Research Institute. He was a Design Engineer with P-Com Inc., USA, and Narda DBS Microwave, USA, in 1998 and 1999, respectively. In 2001, he joined Kyungpook National University, Daegu, South Korea, as a Professor. He is also the Founder of EM-Wise Communications Company Inc., South Korea. His current research interests include microwave communication system and subsystems, microwave and millimeter wave components and packaging, wireless communications, broadband microwave antenna, electromagnetic interaction, and numerical analysis.